Proceedings of the IASS Annual Symposium 2019 - Structural Membranes 2019
Form and Force
7-10 October 2019, Barcelona, Spain
C. Lázaro, K.-U. Bletzinger, E. Oñate (eds.)

From Polyhedral to Anticlastic Funicular Spatial Structures

Mostafa AKBARI[*,a], **Masoud AKBARZADEH**[a], **Mohammad BOLHASSANI**[a,b]

[a] Polyhedral Structures Laboratory, School of Design, University of Pennsylvania, Philadelphia, USA
Pennovation Center, 3401 Grays Ferry ave. Philadelphia, PA, 19146
akbariae@upenn.edu

[b] Bernard and Anne Spitzer School of Architecture, The City College of New York
141 Convent Avenue, New York, NY, 10031

Abstract

The structural performance of cellular polyhedral funicular geometries in 3D graphic statics(3DGS) relies heavily on the buckling performance of the system; if the edges of the form diagram are immediately translated to structural members. In addition, the spatial geometry of the nodes makes the fabrication process quite challenging. This paper proposes a novel approach to translate a cellular polyhedral geometry into a polyhedral surface-based structure in 3DGS that is comparable to the widely known minimal surface geometries in the context of structural design, bridging the gap between cellular polyhedral geometry and surface-based structure. Using such anticlastic structures for materialization in place of polyhedral geometry in 3DGS improves the structural performance of the system and facilitates its fabrications process (Figure 1). The proposed approach introduces a new typology of funicular spatial structures consist of a anticlastic surface for a given boundary condition. Followed by introducing the computational procedure to generate such geometries, the paper concludes by evaluating the mechanical performance of a cellular specimen and a funicular anticlastic surface structure, based on the same polyhedral geometry with the same volume of construction material (see Figure 1).

Keywords: Funicular spatial structure, 3D Graphic statics, Minimal surface, Shell structure

1 Introduction

1.1 Mininal surface geometries and their structural applications

Minimal surfaces are a subset of anticlastic surfaces which have reliable structural performance due to their specific morphology [17].They are surfaces of minimal area between any given boundary conditions which cover the boundary with the least amount of material, weight and area. In nature, we can find such geometries from an equilibrium of homogeneous tension, for instance in a soap film, which have been an inspiration for designers and engineers to expand the borders of light weight structures [9]. At each point on the minimal surface, if we consider k_1 and k_2, the principle curvatures, the mean curvature would be zero ($H = (k_1 + k_2)/2 = 0$) and the Gaussian curvature would be a negative value ($G = k_1 \times k_2 < 0$). If we consider

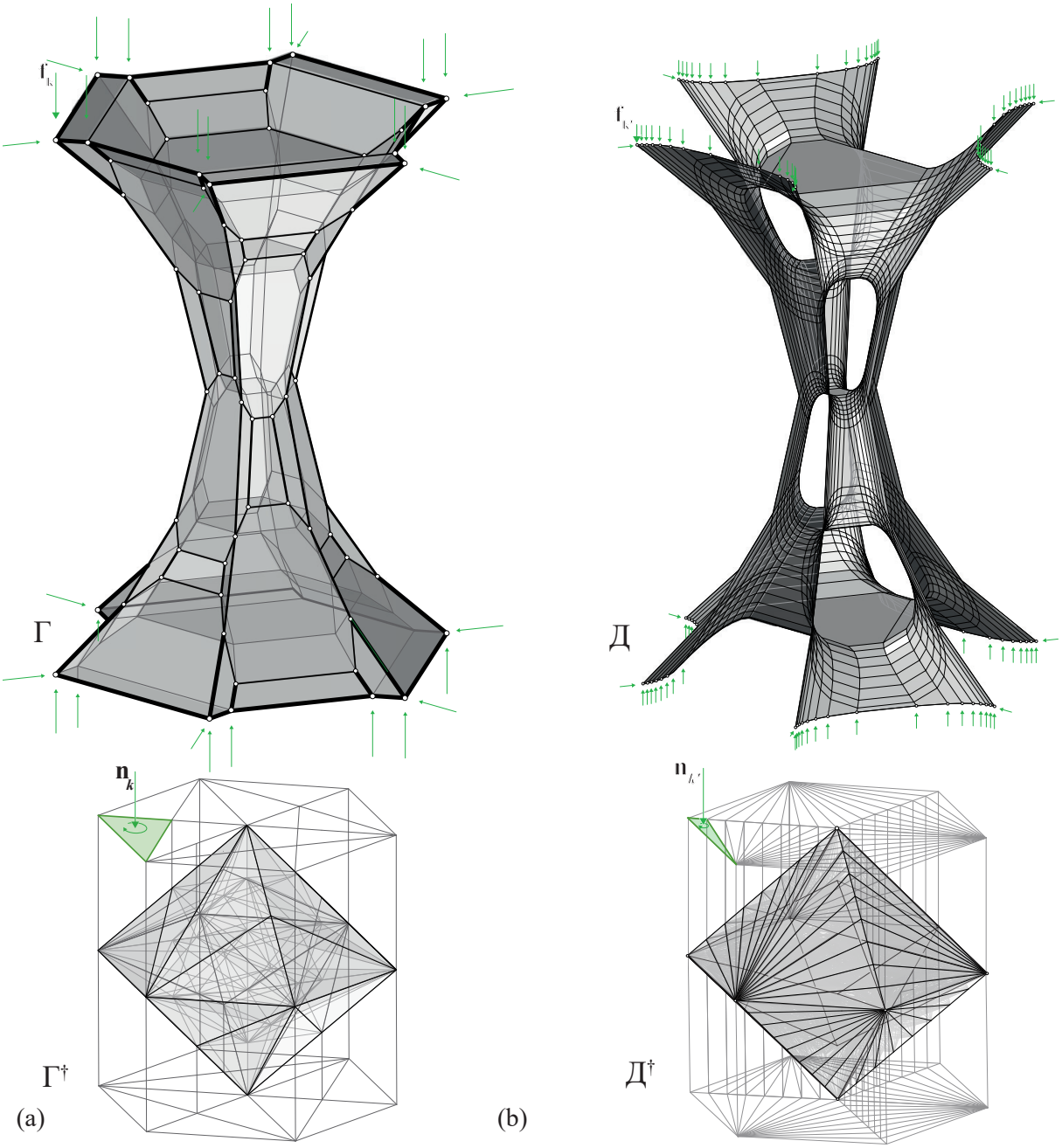

Figure 1: (a) Form and force diagram of a cellular polyhedral specimen in 3DGS; (b) form and force diagram of a translated shellular polyhedral anticlastic surface.

a minimal surface's discretization as a pin-jointed net, at each interior vertex, two edges are curved downwards (standing), and other two curved upwards (hanging) to make an anticlastic curvature on the surface (Figure 3a).

In small scales, minimal surface geometries such as Gyroid, Schwarz P, or Schwarz W are used as space-filling, rigid micro-structures to produce light-weight and high-performance materials [11, 17]. These are two-manifold, single-layer, spatial structures which lately have been named

'Shellular' [10].Recent studies show that the high surface-to-volume ratio in shellular geometries enhances the mechanical performance of the system [10]. Besides, their excelled structural performance are quite useful if used as non-clogging tissue engineering scaffolds or compact light-weight fuel cells with high energy density [10, 20].
Frei Otto was one of the pioneers that utilized mathematical and structural qualities of mininmal surfaces in large scale projects such as German pavilion for expo 1968 and Munich Olympic stadium. Many other architects and engineers also attracted by these surfaces' structural and morphological qualities and used them for the design of light weight structures such as Felix Candela, Sergio Musmeci, and Michael Burt, to name but three [9, 21, 15] (Figure 2).

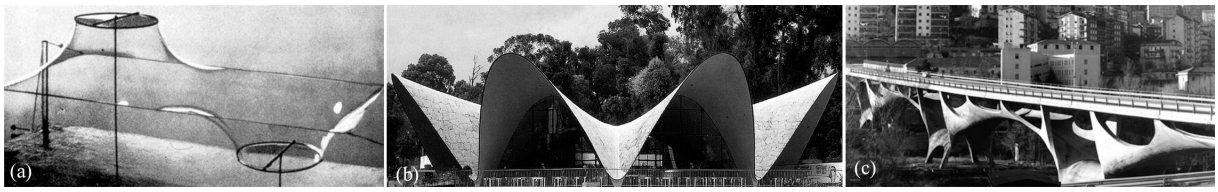

Figure 2: Minimal surface as large-scale structures; (a) Frei Otto's soap film experiment[22], (b) Los Manantiales restaurant by Felix Candela[13], (c) Bridge over the Basento by Sergio Musmeci[5].

1.1.1 Form finding for minimal surface geometries

The geometry of a minimal surface could not be freely chosen and conceived directly, due to the intrinsic interaction between form and forces, and requires a form-finding technique for design application [19, 12] (Figure 2). This process can be applied both in physical or computational method. Frei Otto as one of the pioneers of physical form finding has worked in multiple techniques such as soap film within a boundary or prestressed hanging fabric or cable nets (Figure 2a). The computational methods can be considered both in geometric stiffness family such as Force Density Method (FDM) or in dynamic equilibrium family such as Dynamic Relaxation (DR) or Particle Spring System(PS) [19]. Although a minimal surface's shape can be achieved by finding the shape of equilibrium for an isotropic prestress field with various tools which commonly are based on a method by Pinkall and Polthier [16, 18], there is no geometric method to construct these surfaces for a given set of boundary conditions.

1.2 Problem statement and objectives

Exploring an unlimited variety of funicular spatial structural typologies is now feasible using 3D (polyhedral) graphic statics [1]. These structural forms have polyhedral configurations including vertices, edges, faces, and cells where the edges of the cells can be materialized as members of a structure with a cross section associated with the magnitude of the force (area of the reciprocal face) in the force diagram. The structural performance of cellular polyhedral structures relies heavily on the buckling performance of the members [8]. Besides, if the loading scenario changes, the mechanical behavior of the system will immediately alter. Moreover, the fabrication process of such system is quite challenging because of their complex spatial configurations. Unlike polyhedral systems, minimal surface structures consist of a continuous surface where the internal forces are distributed on a surface with a consistent mean curvature rather than the cross-section of the members. However, the link between the cellular funicular geometry and spatial minimal surface is left unknown.

In this research, we intend to investigate a creative method to design a compression-only, spatial anticlastic surface geometry for a given boundary condition using three-dimensional graphic statics (3DGS).(Achieving a minimal surface geometry happens when the mean curvature in the grometry is zero and this is the next level for this research). Thus, we will; (i) provide a method to generate anticlastic polyhedral geometries using 3DGS ; (ii) describe an approach to generate periodic anticlastic surface geometries as an aggregation of spatial surfaces; (iii) convert a cellular funicular geometry into spatial anticlastic surface geometry for a given boundary condition and applied loads and explain the required computational set up for this purpose; and finally (iv) compare the structural performance of the generated cellular and shellular structures for the same boundary conditions under the applied load using the same volume of material.

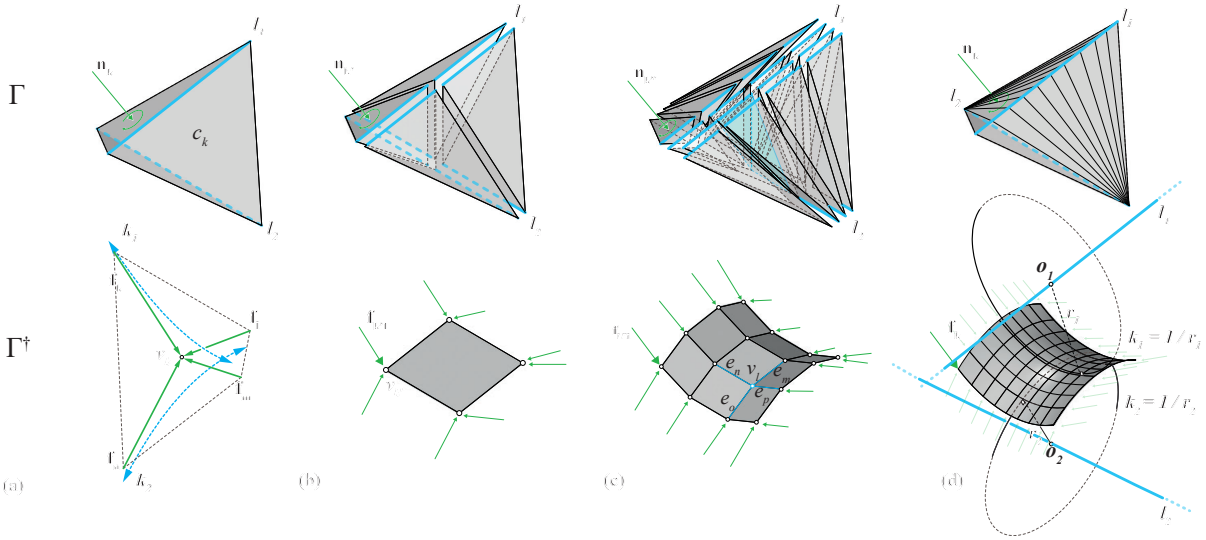

Figure 3: The process of designing an anticlastic surface as a form diagram via subdividing the single polyhedron in the force diagram;(a)single node, (b)4 nodes, (c)16nodes (d)smooth subdivided anticlastic surface with curvatures and axes.

2 Methodology

2.1 Generating anticlastic polyhedral geometry

Subdividing the force diagram as a form finding technique results in a variety of topologically-different structural forms for a given boundary condition and loading scenarios [2, 4]. There are specific types of subdivision rules resulting in a polyhedral surface geometries with synclastic or anticlastic properties. Figure 3 shows a subdivision process that translates a single node in equilibrium into an anticlastic surface. In this process, the two highlighted edges of the global force diagram, l_1 and l_2, are subdivided to construct the surface in each step. Note that in each step of the subdivision, l_1 and l_2 are divided into equal number of segments such that each segment of the former will establish a tetrahedron with its associated segment in the latter (Figure 3b,c). Further subdividing those edges will result in a smoother surface in the form diagram (Figure 3b,c).
However, for this subdivision to work, the force cells should only consist of tetrahedrons. This

results in each node, v_l, on the surface to be connected only to four other nodes with two *hanging* edges, e_n and e_p, and two *standing* edges, e_o and e_m which establishes the negative Gaussian curvature. Moreover, the resulting anticlastic surface of Figure 3 in the form diagram is only subjected to the applied loads from sides with no load applied to the nodes on the surface. As shown in Figure 3c and d, the curvature axis in an anticlastic surface is a subdivision axis in the reciprocal force diagram (l_1 and l_2). More tetrahedron is the direct results of subdivision in the force diagram and subsequently, an smoother anticlastic surface form diagram will be generated as its outcome.

2.1.1 Generating periodic anticlastic surface geometry using 3DGS

Each minimal surface without self-intersection subdivides R^3 into two segregated regions, each of which is connected and forms a 3D labyrinth [6, 7]. The two labyrinths interpenetrate each other with the surface as their common interface. The geometry of the minimal surface changes when the angle of these labyrinth changes. Figure 4 shows the way two skew labyrinths of l_i and l'_i shape the anticlastic surface in between (Figure 4a,b) and how their different angles change the geometry of the anticlastic surface (Figure 4c,d). For instance, according to Figure 4d, axis l_i and l'_i shape surface s_1 in between, while l_i and l'_k shape surface s_2. In fact these two are both part of a bigger surface with same topology but only in different angles.
In 3DGS technique, in a force diagram the angle of subdivisions between the axes can change the geometry of the diagram [3]. According to Figure 4, if we consider l_i and l'_i as anticlastic surfaces' labyrinths, it can be observed that they play the role of subdivision axes in the force diagram ($e^{\dagger}_k || l_i$ and $e^{\dagger}_{k'} || l'_i$) (Figure 4a,c) and the role of labyrinths in the form diagram (Figure 4b,d) which are the surface's curvature axes as well (Figure 3d). For a specific type of anticlastic surface, if we identify the topology of the anticlastic surface by finding its labyrinths, its force diagram can be subdivided based on the labyrinths in order to find the reciprocal funicular geometry in 3DGS.

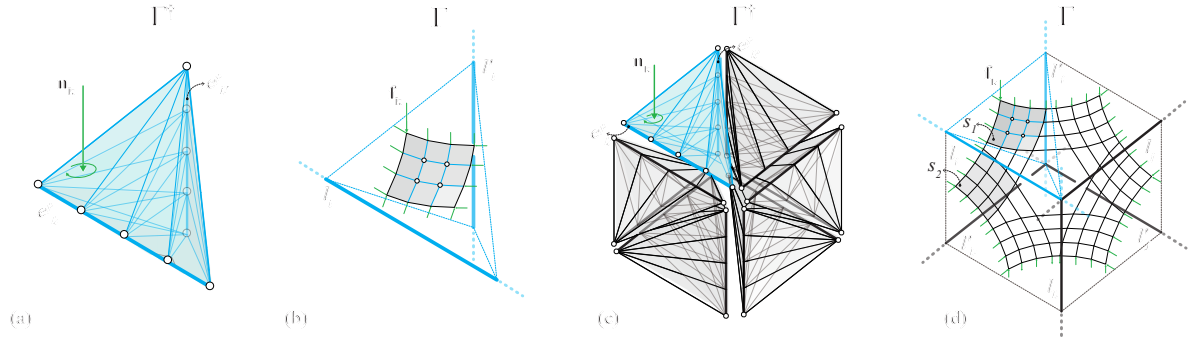

Figure 4: The position of labyrinths in both force and form diagrams of a module of Schwarz P surface, (a) single tetrahedron as force diagram subdivided to 16 tetrahedrons, (b) reciprocal form diagram, (c) Aggregation of the Force diagram, (d) the resulting form diagram of a module of Schwarz P surface.

Similarly, we can explore different aggregations of an anticlastic node to achieve well-known anticlastic surfaces' typologies based on their labyrinths. We designed three types of continuous porous anticlastic surface modules, known as Gyroid(G), Schwarz Premitive(P), and Schwarz iWp(W) (Figure 5). For each surface, for a certain boundary condition in the force diagram

(the cube), the anticlastic surface's labyrinths have been located in the global force and each two skew lines from each groups of labyrinths have been connected together as a tetrahedron (as shown in the Figure 4). Then these tetrahedrons have been subdivided in 3D in order to increase the resolution of the anticlastic surface's form diagram (Figure 5).

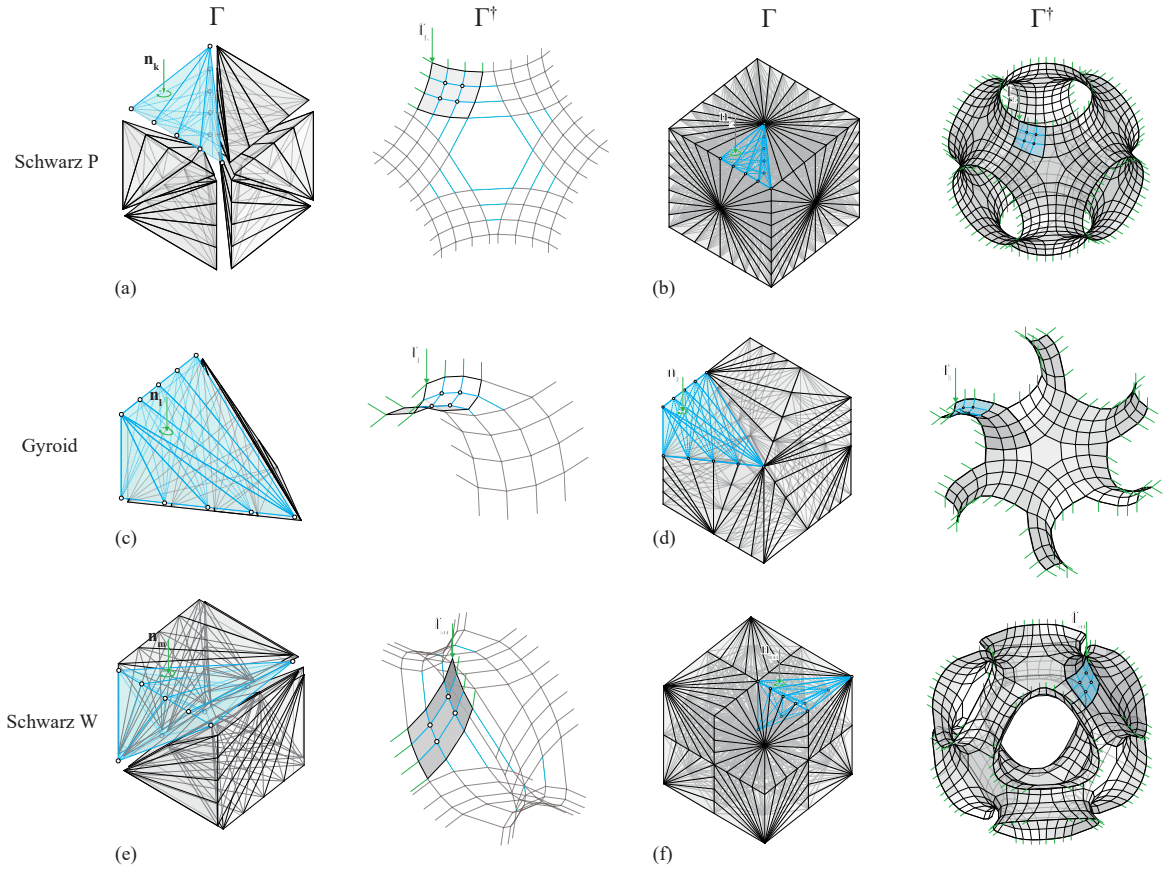

Figure 5: The process of designing three well-known minimal surface modules via 3DGS: (a) force and diagram of a module of Schwarz P surface, (b) force and form diagram of a unit of Schwarz P surface; (c, d) force and form diagrams of Gyroid's surface and its primitive module; (e, f) force and form diagrams of Schwarz W surface and its primitive module.

2.2 Shellular anticlastic surface for a given boundary condition

The ultimate goal of this research is to translate a funicular, compression-only geometry into a compression-only anticlastic surface structure called shellular geometry for the same given boundary conditions and applied loads. For a given polyhedral form, we should find the topology of the two labyrinths that translate the polyhedral form into a continuous surface with two-manifold geometry, dividing the space into two separate sub-spaces. In that case, the topology (connectivity) of these sub-spaces/labyrinths can be used to subdivide the force diagram and generate a shellular version of the cellular form for the given boundary conditions.
We can formulate the problem of finding the labyrinths in the form into the following question: how many faces we can remove from the cellular geometry of the form without removing any

edge from the system such that, at the end, every edge is connected to two and only two faces? The following assumption is necessary for the method to work: *each cell within the polyhedral group should have only and only three-valency vertices.*

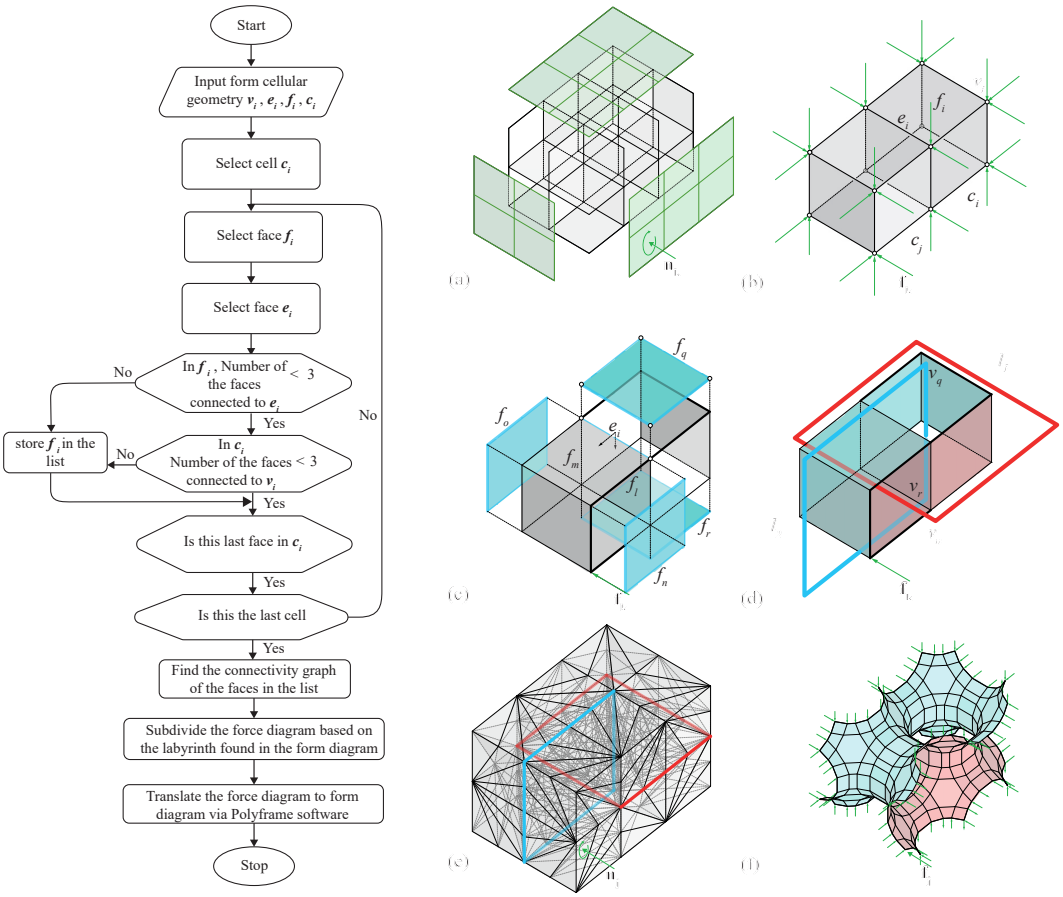

Figure 6: Left; The computational flowchart for translating a cellular spatial structure to funicular anticlastic surface. Right; (a) cellular geometry's force diagram ,(b) cellular geometry's surface-based form diagram, (c) extracting extra faces to make a 2-manifold geometry ,(d) labyrinths, (e) shellular geometry's force diagram, (f) shellular geometry's form diagram.

2.2.1 Computational setup

We can use a brute-force algorithm to find the topology of the labyrinths in the form diagram as explained in the following steps: to tackle the problem, lets start from a single cell in a form polyhedron found for a given boundary conditions [3, 14]. For the first cell c_i, we visit its faces f_{i-n} and store the vertices v_i and edges e_i and remove faces until each edge, e_i is only connected to two and only two faces in the cell (Figure 6c). In this case, each vertex v_i will only be connected to two faces within a cell. In the next step we move to the adjacent cell c_j, where we already have the shared face from the previous cell. Now, we should start by parsing the edges of the shared face, and for each edge of the face, we remove a face of a cell that will make the vertex-face connectivity more than 2 in a cell, and edge-face connectivity more than

2 in whole geometry. By parsing all the cells and removing all the extra faces we will end up with a network of faces that divides the space into two sub-spaces. The connectivity of each sub-space will provide the topology of the labyrinth that should be used to subdivide the force polyhedron to get the shellular funicular geometry (Figure 6a–f).

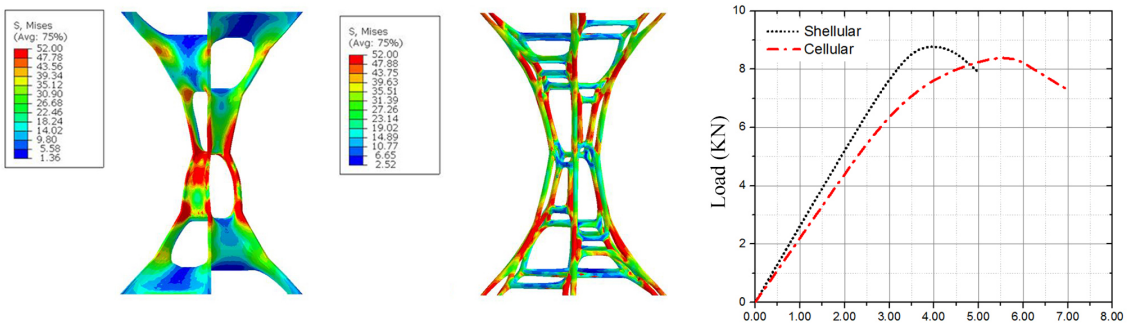

(a) Shellular (b) Cellular (c) Displacement (mm)

Figure 7: (a) Mises stress contour of shellular specimen , (b) Mises stress contour of cellular specimen, (c)Load-displacement curves of cellular and shellular specimens

2.3 Preliminary numerical study

A numerical structural analysis is performed to study the mechanical behavior of two cellular and funicular anticlastic surface structures shown in Figure 1 made out of PLA with identical volume. A tetrahedral meshes consist of approximately half a million elements are generated for both specimens using elastic perfectly plastic behavior with similar boundary conditions, loading speed and type of elements. Although a better performance is expected for the shellular specimen, preliminary load-displacement curves showed that the shellular specimen carry slightly more load and less displacement at the final stage compare to the cellular specimen (see Figure 7). This was mainly due to formation of stress concentration at the sharp edges of the shellular specimen. Mises stress patterns are shown in 7, stress concentration can be observed in the shellular specimen at the sharp edges. On the other hand, maximum stress is distributed along the extend length of members in the cellular specimen.

3 Conclusion and future work

This paper discussed a novel technique to bridge the gap between cellular polyhedral and shellular funicular geometry in 3DGS. We showed that it is possible to generate a shellular polyhedral geometry using 3DGS. Also we showed that shellular funicular geometry is a cellular geometry with particular subdivision that decreases the edge lengths and take advantage of a consistent distribution of internal forces in order to make the geometry structurally reliable and to facilitate the process of fabrication.
It is clear that many aspects of the proposed methodology require further explorations to establish a comprehensive theory of minimal surface funicular spatial structure which could be concerned with optimizing shellular structures load capacity via subdivision, mathematical definition of shellular system in 3DGS, and improving the computational algorithm, to name but a few.

References

[1] M. Akbarzadeh. *3D Graphic Statics Using Polyhedral Reciprocal Diagrams*. PhD thesis, ETH Zürich, Zürich, Switzerland, 2016.

[2] M. Akbarzadeh, T. Van Mele, and P. Block. Compression-only form finding through finite subdivision of the external force polygon. In O. J.B. and R. Tarczewski, editors, *Proceedings of the IASS-SLTE Symposium 2014*, Brasilia, Brazil, 2014.

[3] M. Akbarzadeh, T. Van Mele, and P. Block. On the equilibrium of funicular polyhedral frames and convex polyhedral force diagrams. *Computer-Aided Design*, 63:118–128, 2015.

[4] M. Akbarzadeh, T. Van Mele, and P. Block. Spatial compression-only form finding through subdivision of external force polyhedron. In *Proceedings of the International Association for Shell and Spatial Structures (IASS) Symposium*, Amsterdam, August 2015.

[5] F. CANESTRINI. Ponte musmeci, 1975.

[6] W. Fischer and E. Koch. Genera of minimal balance surfaces. *Acta Crystallographica Section A*, 45(10):726–732, 1989.

[7] W. Fischer and E. Koch. Crystallographic aspects of minimal surfaces. *Le Journal de Physique Colloques*, 51(C7):C7–131, 1990.

[8] A. T. Ghomi, M. Bolhassani, Nejur, and M. Akbarzadeh. The effect of subdivision of force diagrams on the local buckling, load-path and material use of founded forms. In *Proceedings of the International Association for Shell and Spatial Structures (IASS) Symposium 2018*, MIT, Boston, USA, July 2018.

[9] L. Glaeser. *The work of Frei Otto*. The Museum of Modern Art, 1972.

[10] S. C. Han, J. M. Choi, G. Liu, and K. Kang. A Microscopic Shell Structure with Schwarzs D-surface. *Scientific Reports*, 7(1):13405, 2017.

[11] S. C. Han, J. W. Lee, and K. Kang. A new type of low density material: Shellular. *Advanced Materials*, 27(37):5506–5511.

[12] W. Lewis. Computational form-finding methods for fabric structures. *Proceedings of The Ice - Engineering and Computational Mechanics*, 161:139–149, 01 2008.

[13] M. Miller. Los manantiales / felix candela, 1910.

[14] A. Nejur and M. Akbarzadeh. Polyframe beta: a geometry-based structural form finding plugin for rhinoceros3d. https://www.food4rhino.com/app/polyframe, 2018.

[15] F. Otto. *Tensile Structure*. The MIT Press, 1952.

[16] U. Pinkall and K. Polthier. Computing discrete minimal surfaces and their conjugates. *Experimental mathematics*, 2(1):15–36, 1993.

[17] Z. Qin, G. S. Jung, M. Jeong Kang, and M. J. Buehler. The mechanics and design of a lightweight three-dimensional graphene assembly. *Science Advances*, 3:e1601536, 01 2017.

[18] E. Schling, D. Hitrec, and R. Barthel. Designing grid structures using asymptotic curve networks. pages 125–140, 09 2017.

[19] D. V. C. W. Sigrid Adriaenssens, Philipe Block. *Shell structures for architecture, form finding and optimization*. Routledge, 2014.

[20] B. Trembacki, E. Duoss, G. Oxberry, M. Stadermann, and J. Murthy. Mesoscale electrochemical performance simulation of 3d interpenetrating lithium-ion battery electrodes. *Journal of The Electrochemical Society*, 166:A923–A934, 01 2019.

[21] L. Velimirovi, G. Radivojevi, M. Stankovi, and D. Kostic. Minimal surfaces for architectural constructions. *Facta Universitatis - series : Architecture and Civil Engineering*, 6, 01 2008.

[22] S. Zexin and H. Mei. Robotic form-finding and construction based on the architectural projection logic. *IOP Conference Series: Materials Science and Engineering*, 216:012058, 06 2017.